Undergraduate Journal of Experimental Microbiology and Immunology (UJEMI) Vol. 27:1-15

Testing the functionality of SIGEX duo-directional reporter plasmid pSPPH21 using an inducible promoter

Sarah Agnew, Alexis Bangayan, Joanne Fan, Amy Lin

Department of Microbiology and Immunology, University of British Columbia, Vancouver, British Columbia, Canada

SUMMARY The bidirectional, promoterless vector pSPPH21 constructed by Abrishamkar et al. features the fluorescence reporter genes, GFP and RFP flanking a NruI restriction enzyme site. Although the presence of the reporter genes in the vector were confirmed via sequencing with a few point mutations in the upstream region of the GFP reporter gene, the functionality of pSPPH21 as a reporter vector has not been elucidated. Thus, in this study, the reporting ability of the pSPPH21 vector will be tested by cloning in a T7-*lac* inducible promoter system and inducing with an IPTG substrate. A lac operator (*lacO*) constitutively active mutant was also constructed. The responsiveness of the fluorescent reporting genes in the presence of a metabolic substrate can now be tested alongside the plasmid functionality. However, only recombinant pSPPH21 plasmids with the T7 promoter insert in the orientation specific to the GFP reporter gene were generated. Fluorescence emissions by IPTG induction indicate the downstream GFP reporter gene is responsive to upstream gene inserts. This confirmed that the point mutations in the upstream region of the GFP reporter gene does not affect the reporting ability of pSPPH21. The GFP fluorescent emissions generated through IPTG induction of the ligated T7 promoter provides supporting evidence that the constructed bidirectional vector pSPPH21 is functional in the GFP reporter gene orientation. However, the generated inserts also had levels of fluorescent gene expression without induction, which imply that there is an extremely high affinity of the T7 RNA polymerase to the constructed T7 promoter sequence regardless of induction. No clones generated any RFP expression, thus no conclusions can be made regarding its functionality in pSPPH21. The pT7Mut colonies were revealed to contain no T7Mut promoter insert and thus, no fluorescence activity. Therefore, no conclusions can be made whether the promoter is constitutively activated. Design optimizations of inducible promoters to create more functional clones in order to further validate the GFP and RFP functionality and orientation bias of pSPPH21 is recommended.

INTRODUCTION

The screening of metagenome libraries and isolation of novel genes typically utilize substrate-induced gene-expression (SIGEX) techniques (1). More specifically, SIGEX is commonly used to study coordinately expressed gene-pairs, or genes that are regulated and induced by metabolic substrates (1). SIGEX experiments typically use promoter trapping, an approach that features a promoterless single fluorescence reporter system that only activates expression in the presence of certain substrates for selection of positive clones (2). This system relies on the insertion of a promoter in the specific orientation that will result in the simultaneous expression of the reporter gene downstream once induced by the respective substrates (2). As such, the unidirectional design of SIGEX vectors prevents the detection of genes inserted in the reverse direction (3). Furthermore, increasing amounts of research have shown that there are single promoter sites which confer transcription in both forward and reverse directions (4). Duo-directional plasmid vectors have been designed to overcome this limitation. These vectors are equipped with reporter genes in both orientations to detect genes of interest inserted in either direction (3). Abrishamkar et al. designed a SIGEX vector, pSPPH21, featuring a secondary reporter gene oriented in the reverse direction to circumvent the conventional obstacles associated with single-reporter gene vector constructs (3). This promoterless, bidirectional plasmid vector pSPPH21 incorporates two reporter genes: red

Published Online: September 2022

Citation: Sarah Agnew, Alexis Bangayan, Joanne Fan, Amy Lin. 2022. Testing the functionality of SIGEX duo-directional reporter plasmid pSPPH21 using an inducible promoter. UJEMI 27:1-15

Editor: Andy An and Gara Dexter, University of British Columbia

Address correspondence to: https://jemi.microbiology.ubc.ca/

fluorescent protein (RFP) and green fluorescent protein (GFP) (3). These fluorescence elements enable the detection of gene expression in the forward and reverse directions.

Additionally, pSPPH21 harbors a single NruI restriction enzyme site in between the RFP and GFP genes, for blunt-end ligation of metagenomic DNA with any promoter system (3). The advantage of blunt-end ligation in a bidirectional vector is that promoters can be ligated in any direction and will still be reported by the fluorescent reporters. Furthermore, the duo reporting system may be useful in future high-throughput screening of the emerging divergent promoter groups (4). Abrishamkar et al. previously confirmed the pSPPH21 construct harbors two reporter genes flanking the NruI site; however, its functionality is yet to be validated (3). They also determined that there are point mutations in the ribosomal binding site of the GFP gene (3). Thus, elucidating the ability of pSPPH21 as a duo-directional reporter plasmid, while also mindful of the mutations, is the appropriate next stage of experimental testing.

The T7 promoter is a common and well-known inducible promoter typically inserted upstream of fluorescent reporter genes in protein expression studies. These promoter systems originated from T7 bacteriophages, where their highly-regulated promoter and polymerase system have been isolated for their ability to express genes that are ligated downstream (5). It has been shown that the T7 RNA polymerase is effective in redirecting the metabolism in *Escherichia coli (E. coli)* strains to focus on synthesizing the T7 phage particles, which is largely what the T7 promoter-based system exploits in protein expression studies (6). This system can use isopropyl-B-D-thiogalactoside (IPTG) substrate to induce protein expression (7). *E. coli* BL21(DE3) contains the essential T7 RNA polymerase to activate the T7 promoter, making it an ideal host for protein expression studies (8). Furthermore, due to its high affinity and efficiency, the T7 RNA polymerase can induce the over-expression of any gene sequences regulated under the T7 promoter (6). As such, a T7 promoter-based system, specifically of the *lac* operon, will be utilized in generation of recombinant pSPPH21 plasmids alongside the substrate IPTG to test the functionality of the constructed vector. Induction with IPTG should simultaneously induce the expression of the fluorescent reporter genes and enable high-throughput screening methods to select for positive clones.

The responsiveness of a recombinant pSPPH21 plasmid featuring the T7-*lac* promoter will be compared to a constitutive mutant of the same operon. It has been proposed that mutations nearing the 5' region of *lacO* within the T7-*lac* promoter construct reduces the repressor affinity, enabling constitutive gene activity (9). Thus, this study will focus on using T7-*lac* promoter (T7) and T7 mutated *lacO* (T7Mut) ligated into the pSPPH21 vector to create the recombinant plasmids pT7 and pT7Mut, respectively. Ligations will be executed via blunt-end ligation and subsequently transformed into *E. coli* BL21(DE3) to test the pSPPH21 functionality.

In this experiment, blunt-end cloning performed destroying the NruI cut site is expected to increase the ligation efficiency of the T7 and T7Mut promoter insert into the pSPPH21 vector. In other words, blunt-end ligation is expected to minimize the probability of empty vector recircularization and promote the ligation of the plasmid with the designated T7 and T7Mut inserts. Ligations will be confirmed through the linearization of the recombinant vectors using an HindIII restriction enzyme site incorporated within the design of T7 and T7Mut promoter inserts. Recombinant plasmid linearization will be resolved by gel electrophoresis to confirm the presence of the inserts in pSPPH21 prior to protein expression studies in *E. coli* BL21(DE3). The induced GFP and RFP gene expression levels can then be quantified and assessed to draw conclusions on the functionality of the novel duo-directional reporter plasmid pSPPH21.

METHODS AND MATERIALS

Inducible Promoter Design and Preparation

Two pairs of 5' phosphorylated reverse complementary primers were designed *in silico* and ordered from Integrated DNA Technologies (IDT). Both pairs contained the T7 promoter and *lacO* genes, followed by a HindIII restriction enzyme site for colony screening (SnapGene). To generate constitutive expression in T7Mut, three base pairs were mutated in the *lacO* region (Table S2). Duplex buffer (100 nM potassium acetate, 30 nM HEPES, pH 7.5) was used to rehydrate primers to a final concentration of 100 μM. Forward and reverse primers were annealed in a 1:1 ratio to generate final concentrations of 25 μM and 50 μM by heating

at 94°C for 2 minutes, followed by cooling at room temperature for 60 minutes (10). Gel electrophoresis of pre-annealed and annealed primers were run as specified in "Agarose DNA Gel Electrophoresis".

Bacterial Strain and Media Preparation

E. Coli DH5α and BL21(DE3) cultures were obtained from MICB 401 lab starter plates. The cultures were grown in Lysogeny Broth (LB) (0.01 g/mL tryptone, 0.005 g/mL yeast extract, 0.01 g/mL NaCl, distilled water). Agar plates were prepared by adding 15 g of agar per liter of LB (11). Chloramphenicol (chlor) antibiotic (25 mg/mL powdered chlor in 95% EtOH) was added to LB agar and LB liquid after sterilizing via autoclave for a final antibiotic concentration of 25 µg/mL.

Competent Cell and Plasmid Preparation

Overnight cultures of *E. Coli* DH5α and BL21(DE3) were subcultured until an approximate OD_{600} of 0.5 was achieved. Calcium chloride working solutions (0.1 M $CaCl_2$, 15% glycerol) were prepared and used to resuspend competent cells of both strains (12). The pSPPH21 plasmid was obtained from a frozen stock of transformed *E. coli* DH5α from Abrishamkar et al. where cultures were grown in a shaking incubator at 37°C overnight. Plasmid minipreps were done using the alkaline lysis method via EZ-10 Spin Column Plasmid DNA Minipreps Kit for high copy number plasmids (BioBasic). DNA concentration and purity was assessed using a NanoDrop2000® Spectrophotometer using the nucleic acid setting (ThermoFisher). Subsequent plasmid isolations were completed using the same procedure.

Digestion and Dephosphorylation of pSPPH21

Approximately 1 µg of pSPPH21 was digested with 20 units of NruI, CutSmart Buffer (NEB), and nuclease free water at 37°C for 1 hour. A negative control without NruI was prepared using 0.5 µg plasmid DNA. The reactions were heat inactivated at 80°C for 20 minutes (13). Digested pSPPH21 was dephosphorylated by incubating with 10 units of Antarctic Phosphatase (AP) and AP reaction buffer at 37°C for 30 minutes. The reactions were heat inactivated at 80°C for 2 minutes (14). Gel electrophoresis of treatment and control was run as specified in "Agarose DNA Gel Electrophoresis".

Ligation of Inserts into pSPHH21

The first ligation attempt was a 1:3 ratio of NruI digested pSPPH21 vector and the double-stranded duplex insert. The ligation mixtures for the T7 and T7Mut promoters contained the following: 1X T4 ligase (ThermoFisher), 1X T4 ligase buffer (ThermoFisher), 198-216 ng insert, 66-72 ng digested vector, and nuclease-free water to a total reaction volume of 20 µL. The ligation mixtures were incubated at room temperature for 2 hours, followed by heat inactivation at 65°C for 10 minutes. The ligation mixture was chilled on ice and eventually stored at -20°C for future transformation.

The second ligation attempt was prepared as per the first attempt, with the appropriate vector to insert ratio substitutions as follows: 3.6 to 72 ng, 8.4 to 72 ng, and 14.2 to 72 ng, for the ratios 1:3, 1:7, and 1:12, respectively. The ligation mixture was incubated overnight at 20°C and subsequently heat-activated at 65°C for 10 minutes. The ligation mixture was cooled on ice and then stored at -20°C for future transformation. Ligation control reactions were subjected to the same treatment, with the following varying compositions: linear vector without ligase, linear vector with ligase, and insert with ligase.

Transformation of Recombinant Plasmid into *E. coli* DH5α and BL21(DE3)

E. coli DH5α competent cells were transformed with the prior ligation reactions using the heat-shock method (12). Untransformed *E. coli* DH5α competent cells were spread on a LB agar plate with no antibiotics as a positive control and to check for cell viability. The untransformed *E. coli* DH5α competent cells were spread on a LB agar plate with chlor antibiotic (25 µg/mL) as a negative control. The transformed cells were also spread on LB agar plates with chlor antibiotic (25 µg/mL) as selective pressure, and incubated overnight at 37°C. Positive transformants were selected from these plates, streaked onto new LB agar plates with chlor antibiotic (25 µg/mL), then incubated overnight at 37°C to create master

plates of each colony. Colonies from the master plates were used to inoculate overnight cultures, where plasmids of the positive clones were then purified. Nanodrop and gel electrophoresis of the purified plasmids were performed to assess the DNA concentrations and quality, respectively.

Transformation of *E. coli* BL21(DE3) with the purified plasmids from *E. coli* DH5α was subsequently performed, following the same heat-shock method and subsequently spread on LB agar with chlor antibiotic (25 µg/mL) as previously done (12). *E. coli* BL21(DE3) competent cells with no plasmid were spread on LB agar and LB agar with chlor antibiotic (25 µg/mL) as a positive and negative control, respectively. Plates were incubated overnight at 37°C. The positive clones following transformation were streaked on LB agar with chlor antibiotic (25 µg/mL) as master plates. Colonies from the master plates were used for downstream analyses of the transformants, presumed to contain the recombinant pSPPH21 plasmid, via plasmid preparations, gel electrophoresis, and Sanger sequencing.

Agarose DNA Gel Electrophoresis

Gel electrophoresis was performed for isolated recombinant plasmid clones from transformed *E. coli* DH5α and *E. coli* BL21(DE3). DNA concentration of vectors was calculated based on NanoDrop2000® spectrophotometer readings at 260 nm (ThermoFisher). Isolated plasmids from each colony and the empty vector pSPPH21 were linearized with restriction enzyme HindIII, with each reaction mixture containing the following: 1 µg of plasmid vector, 2 µL 10X Buffer R, 1 µL HindIII (10 U/µL), 16 µL nuclease-free water. The reactions were incubated at 37°C for 1 hour, followed by an 80°C heat block for 20 minutes. Negative controls included the isolated colonies and empty vector pSPPH21 containing no HindIII enzyme in the reaction mixture. Gel electrophoresis using 1.0 % agarose gels 1.0 g/mL UltraPure ® Agarose Powder (ThermoFisher), 1X TAE buffer, 5 uL RedSafe Nucleic Acid Stain (ThermoFisher) was performed to resolve the DNA band sizes. DNA samples containing 20-200 ng of DNA and 1kb Plus Ladder (Invitrogen) were mixed with 6X NEB purple sample loading buffer prior to loading onto the gel. The gels were run at 130-150V for 60 minutes. Imaging was performed using an ultraviolet (UV) gel imaging system (BioRad) on the SYBR DNA detection setting.

Sanger Sequencing of Recombinant Plasmids

Previously isolated recombinant plasmid DNA from pT7 and pT7Mut DH5α transformants were outsourced to GeneWiz for Sanger sequencing. Primers designed to bind upstream of RFP (forward) and downstream of GFP (reverse) were obtained from Abrishamkar et al. (Table S2). Samples were prepared using aliquots of 500 ng of plasmid DNA in 10 µl volumes, and 25 pmol of forward and reverse primers in 5 µl volumes were prepared separately. Sequence alignment and analysis was done on CLC Genomics software. Forward and reverse sequences were aligned and compared to T7 and T7Mut inserts as a reference sequence.

Additional primers, pT7FP and pT7RP, were designed *in silico* closer to the insert site to achieve higher resolution sequencing results. The primers were designed to be approximately 100 base pairs (bp) away from the NruI site, contain a melting point of 55-60°C, and a G/C content of 40-45% (Table S2). Isolated recombinant plasmid DNA from *E. coli* BL21(DE3) transformants were outsourced to GeneWiz for Sanger sequencing using the pT7FP and pT7RP primers. Samples were prepared and analyzed under the same conditions as previously done.

IPTG Induction

IPTG substrate was utilized to induce the GFP and/or RFP fluorescence expression of *E. coli* BL21(DE3) transformed clones containing the recombinant pSPPH21 plasmid. Two different methods of IPTG induction methods were performed to assess the fluorescence activity of the plasmid reporter: 1) fast IPTG induction (15), 2) overnight IPTG induction.

For the fast IPTG induction method, 1 mL of pT7 and pT7Mut BL21(DE3) overnight cultures were inoculated into 1 mL LB with chlor (25 µg/mL) with or without 0.5 mM IPTG substrate for control and induced treatments, respectively. The samples were incubated on a

shaker at 37°C for 3 hours and subsequently spun at max speed for 30 seconds at room temperature. Pellets were stored at -20°C until needed for fluorescence analysis.

For the overnight IPTG induction method, the following IPTG (mM) concentrations were used to induce fluorescence expression: 0.5, 0.25, 0.125, 0.0625. LB with chlor antibiotic (25 µg/ul) was plated in a 96-well plate, with treatment wells containing the corresponding IPTG concentrations. Culture volume of pT7 or pT7Mut BL21(DE3) overnight cell cultures were loaded into the wells in a 1:40 ratio and in duplicates. The 96-well plate was incubated with orbital shaking at 37°C in a BioTek microplate reader for 20 hours, taking OD_{600} every hour timepoint.

Assessing GFP and RFP Expression

The GFP and RFP expression of clones were read on a fluorescence 96-well plate reader. For fast IPTG induction frozen pellet samples, the pellets were thawed, washed twice, and resuspended with PBS (8 mg/mL NaCl, 0.2 mg/mL KCl, 1.1 mg/mL Na_2HPO_4, 0.2 mg/mL KH_2PO_4, distilled H_2O, pH 7.4) to prepare for reading. Samples were diluted 1:4 and plated in duplicate into a 96-well plate, using PBS as blanks. For the overnight IPTG induction, the 96-well plate was immediately read after the 20-hour end-point incubation time. GFP readings were done on excitation and emission wavelengths of 485 nm and 528 nm, respectively. RFP readings were done on excitation and emission wavelengths of 488 nm and 588 nm, respectively. OD_{600} end-point readings from the overnight culture were used to normalize the GFP and RFP readings from the fluorescence plate reader.

A preliminary visual assessment for leaky GFP expression of uninduced *E. coli* BL21(DE3) transformants and subsequent master plates were performed using an ultraviolet (UV) gel imaging system (BioRad) on the Alexa 488 Blot detection setting.

RESULTS

Oligomer primers used to create T7 and T7Mut promoters were annealed into duplexes.

In order to clone an inducible promoter to test the functionality of pSPPH21 plasmid, primers were designed and annealed to behave as T7 inducible promoter inserts. The primer design of the inducible promoter includes the T7 promoter, *lacO*, and HindIII cut site (Figure 1A, Table S2). A HindIII cut site was incorporated in the insert for ease of downstream screening experiments. The constitutively active T7Mut promoter shared the same sequence except 3 base substitutions in the *lacO* sequence (Figure 1B, Table S2). Primer controls did not undergo the annealing operations and were expected to be single-stranded. Annealed oligos and primer controls both resolved at the molecular weights (MW) below 250 bp (Figure S1). These DNA fragments were too small to compare against the kb ladder, which is expected from the constructed 50 bp oligos (Figure S1). The annealed oligos had a slightly lower MW band compared to primer controls, which was expected due to being a double-stranded compact duplex compared to the single-stranded primer controls (Figure S1). Thus, the lower MW band of annealed oligos suggests that the complementary oligos were annealed as double-stranded duplexes and ready to perform as T7 inducible promoter inserts.

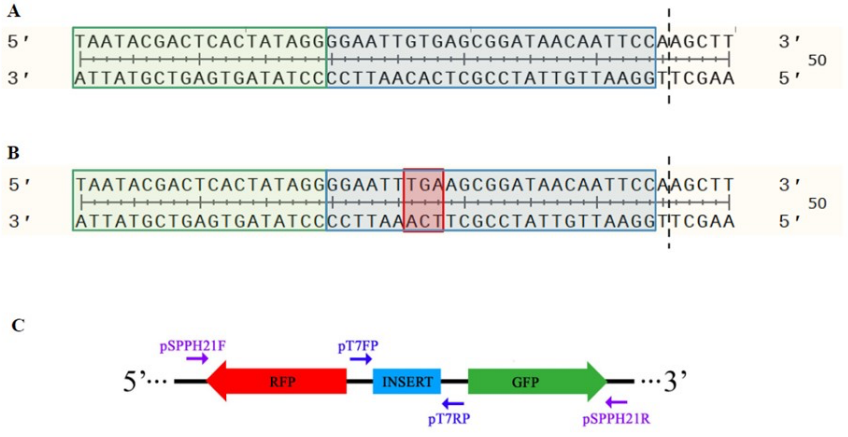

FIG. 1 Graphical depiction of the T7 inducible promoter (**A**), the T7Mut constitutive promoter (**B**), and a section of the recombinant pSPPH21 plasmid (**C**). For panels (**A**) and (**B**), the green box indicates the T7 promoter sequence; the blue box indicates the *lacO* sequence; the red box indicates the 3bp mutation on the *lacO*; the dash lines indicate the HindIII cut site. For panel (**C**), pSPPH21F/R primers were designed by Abrishamkar, et al. pT7FP/RP self-designed. Image does not represent the true size of insert and genes.

Low efficiency ligation of digested pSPPH21 vector and T7 promoter insert by blunt-end cloning.

In order to generate recombinant pSPPH21 plasmids with T7 or T7Mut inducible promoters, linearized pSPPH21 vector by NruI digestion was ligated with corresponding T7 inducible promoter inserts, and subsequently transformed into *E. coli* DH5α competent cells (Figure 1C). Negative ligation negative controls included linear vector without ligase, linear vector with ligase, and insert with ligase to assess the efficiency of digestion or re-ligation of plasmid during ligation reaction. Positive transformation clones were screened using LB with 25 μg/ml chlor spread plates, while competent DH5α cells were plated on both LB with and without 25 μg/ml as positive and negative controls, respectively. Ligation conditions with the molar concentration ratio 1:3 of vector to duplex insert was the most optimal condition for ligation efficiency. The other molar concentration ratios did not produce any colonies. Furthermore, different incubation conditions did not increase the ligation efficiency as both conditions only produced a maximum of two colonies per treatment. In general, both ligation conditions demonstrated minimal transformants which were further screened for the presence of corresponding inserts via gel electrophoresis and Sanger sequencing. Following the transformation of the positive recombinant plasmids into *E. coli* DH5α, the same plasmids were transformed into *E. coli* BL21(DE3) cells.

High transformation efficiency was observed on LB agar with chlor spread plates of transformed cells, as assessed by colony forming units being too numerous to count (CFUs).

Gel electrophoresis of HindIII digested plasmids demonstrated ligation for pT7 DH5α and BL21(DE3) clones.

In order to confirm the presence of the T7 inducible promoter insert in the transformants from *E. coli* DH5α and BL21(DE3) cells, plasmids isolated from pT71 DH5α colony and pT71 BL21(DE3) colonies 1-5 were digested with HindIII and screened on a 1% agarose gel electrophoresis (Figure 2). Controls included: undigested pSPPH21 vector, digested pSPPH21 vector, and undigested pT7 recombinant plasmids. Notably, the digested empty vector had a different MW band size compared to the undigested empty vector (Figure 2A). The unexpected cut by HindIII in the empty vector suggests there are other HindIII cut sites within the pSPPH21 vector other than the designed insert (Figure 2). Digested pT7 recombinant plasmids isolated from DH5α and BL21(DE3) colonies demonstrated distinct linear bands approximately 3200 bp, which is approximately the expected size of the recombinant plasmid (Figure 2, Figure S4). In contrast, the undigested recombinant plasmid controls showed multiple smeared bands, indicating nicked, linear, and supercoiled forms of the plasmid (Figure 2). As a result, the comparison of cut and uncut pT7 plasmids suggests that the HindIII enzyme was functional (Figure 2). Notably, the digested pT7 plasmids ran further down the gel compared to the digested empty vector, indicating that the pT7 linearized plasmids are lighter in size (Figure 2). This is likely due to the additional HindIII site, leading to more fragments generated after HindIII digest. Thus, the HindIII digest and gel electrophoresis screen suggests that the T7 inducible promoter insert was ligated into the pSPPH21 plasmid.

Gel electrophoresis of HindIII digested plasmids demonstrated failed ligation for pT7Mut1 and pT7Mut2 clones from DH5α and BL21(DE3).

To confirm the presence of T7Mut inducible promoter insert in the transformants from DH5α and BL21(DE3) cells, plasmids isolated from pT7Mut1 and pT7Mut2 DH5α colonies, and pT7Mut1 BL21(DE3) colony 1-2 were digested by HindIII and resolved using 1% agarose gel electrophoresis. Controls included: undigested pSPPH21 vector, digested pSPPH21 vector, and undigested pT7Mut recombinant plasmids. All pT7Mut colonies in both DH5α and BL21(DE3) had distinct linear bands near 3500 bp (Figure 2). As expected, the undigested pT7Mut controls showed at least 2 smeared bands (Figure 2A). As discovered, the empty vector also exhibited cutting from the HindIII restriction enzyme (Figure 2A). Interestingly, the digested empty vector and digested pT7Mut MW bands were very similar, both having a MW of 3500 bp and were slightly heavier than previous pT7 bands (Figure 2). This observation suggests that the pT7Mut colonies most likely contained empty vectors, therefore no ligation of the pT7Mut inserts into the pSPPH21 plasmids occurred.

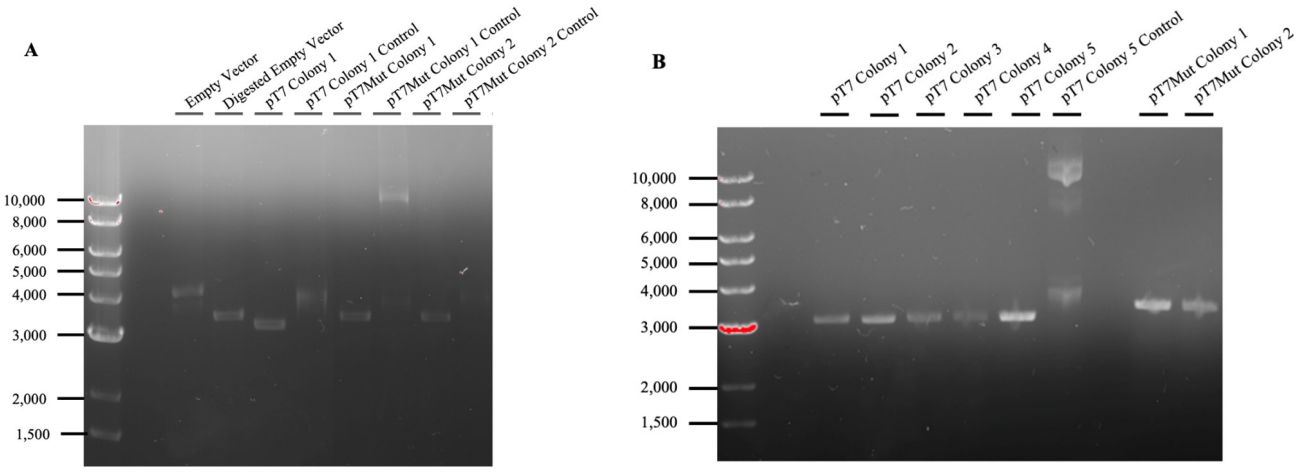

FIG. 2 Gel electrophoresis of plasmids extracted from candidate DH5α (**A**) or BL21(DE3) (**B**) colonies transformed with pT7 or pT7Mut. Plasmids were run after HindIII digestion and undigested as a negative control. **A**) An additional negative control of HindIII digested pSPPH21 (empty vector) was run. 1% agarose gels were prepared with SYBR Red and run with a 1kB plus DNA ladder (Invitrogen). Gels were run at 130-150V for approximately 60 minutes and imaged using GelDoc UV imaging system (BioRad).

Sequencing results confirmed the presence or absence of promoters following ligation into the pSPPH21 vectors in pT7 and pT7Mut DH5α colonies.

Following the gel electrophoresis results (Figure 2A), Sanger sequencing was performed to confirm the presence and orientation of the T7 inducible promoter in the isolated vector of the pT71 DH5α colony. Analysis of the sequencing results from the pSPPH21F forward primer results does not clearly show the presence of the T7 promoter due to the number of unidentified nucleotides ('N') located at approximately 820 base pairs (Figure 3A). However, the sequencing results from the pSPPH21R reverse primer revealed the presence of the full T7 promoter that was inserted in the NruI site. This was located at approximately 850 base pairs (Figure 3B) in the same 5' → 3' orientation as the GFP sequence. The pSPPH21R results overlap with the full T7 promoter sequence on the pT7 reference (Figure 3B). This suggests the isolated vector from the pT71 DH5α colony contains the T7 promoter ligated into the pSPPH21 backbone vector in an orientation that allows the expression of GFP when transformed into BL21(DE3). Additionally, the sequencing results from isolated vectors of pT7Mut1 and pT7Mut2 DH5α colonies revealed an intact NruI site and the absence of the T7Mut promoter (Figure 3). Thus, the pT7Mut DH5α colonies only contained the pSPPH21 backbone sequence without the insert, which agrees with the gel electrophoresis results (Figure 2).

Sequencing results confirmed the partial presence or absence of promoters following transformation of DH5α isolated vectors into BL21(DE3) cells.

The previous sequencing results show poor sequencing quality at the location of the insert (Figure 3). Thus, new primers (T7FP, T7RP) were used in sequencing of the pT71 BL21(DE3) colonies 1-4 to confirm the presence of the T7 promoter insert in these vectors. According to the gel electrophoresis results (Figure 2B), the pT71 BL21(DE3) colonies 1-4 appear to have the T7 promoter ligated. Future GFP expression studies also showed GFP expression for these colonies, which suggests there was proper ligation of the T7 promoter in the same 5' → 3' orientation as the GFP sequence (Figure 4B-E, Figure 5).

The sequencing quality was good at the expected location of the T7 promoter (Figure S3). However, the sequence results demonstrated that pT71 BL21(DE3) colonies 2 and 3 only contained the HindIII site of the T7 promoter (5'-AAGCTT-3') flanked between the NruI sites (Figure S3A). The pTT71 BL21(DE3) colony 4 contained the *lacO* sequence (5'-GGAATTGTGAGCGGATAACAATTCC-3') and HindIII site sequence, but lacked the T7 promoter sequence (Figure S3A). An additional HindIII site was found directly upstream of

A

```
pT71_DH5a_For          tgaactctttgataacgtcttcggaggaagccattactagagtttctcctctttaatTCG   1740
pT7_For_reference      TGAACTCTTTGATAACGTCTTCGGAGGAAGCCATTACTAGAGTTTCTCCTCTTTANTCNN   759
                       ******************************************************* *

pT71_DH5a_For          TAATACGACTCACTATAGGGGAATTGTGAGCGGATAACAATTCCAAGCTTCGAattaaag   1800
pT7_For_reference      NNTTNTGGNANTNGTTNNNCGGNTNNCNATTCCANGATTNNNTNNNNNTNNCAANNTGGG   819
                          *  *        *    *  *    *    *  *          *   **     *

pT71_DH5a_For          aggagaaaTACTAGAGatgcgtaaaggagaagaacttttcactggagttgtcccaattct   1860
pT7_For_reference      AANNNNNAGCGNANAN--------NNNNGCANGANNTGANACTAGANTNNCAACNGAAAG   871
                            *      *    * *            * *  *  *   *** ** *     *

pT71_DH5a_For          tgttgaattagatggtgatgttaatgggcacaaattttctgtcagtggagagggtgaagg   1920
pT7_For_reference      -----NNGTAGATGCNNNANNNANNNN-------------------------------   893
```

B

```
pT71_DH5a_Rev          tgcccattaacatcaccatctaattcaacaagaattgggacaactccagtgaaaagttct   1740
pT7_Rev_reference      TGCCCATTAACATCACCATCTAATTCAACAAGAATTGGGACAACTCCAGTGAAAAGTTCT   779
                       ************************************************************

pT71_DH5a_Rev          tctcctttacgcatCTCTAGTAtttct----cctctttaatTCGAAGCTTGGAATTGTTA   1796
pT7_Rev_reference      TCTCCTTTACGCATCTAGTACTTTCCTGTGTGACTCTAGTATCGAAGCTTGGAATTGTTA   839
                       ****************      ** **         *    ******************

pT71_DH5a_Rev          TCCGCTCACAATTCCCCTATAGTGAGTCGTATTACGAattaaagaggagaaactctagta   1856
pT7_Rev_reference      TCCGCTCACAATTCCCCTATAGTGAGTCGTATAAAANNTNGNANNNNNNNNNNCNNN---   896
```

FIG. 3 Sequencing results of the vector isolated from a pT71 DH5α colony aligned with the pT7 reference sequence using the Clustal Omega tool, in the forward (**A**) and reverse (**B**) orientation. The top line contains the sequence of the pT7 reference which is the pSPPH21 vector with the inducible promoter sequence inserted in a 5' → 3' orientation flanked by the NruI sites. The bottom line contains the isolated and sequenced vector of the pT71 DH5α colony. The underlined letters indicate the NruI site. The bolded letters indicate the inducible promoter sequence (5' → 3'). The ⋆ indicates a match between the bases, while a lack of this indicates a mismatch between the bases. The horizontal lines indicate gaps in the sequence alignment. The letter 'N' represents regions where the bases could not be not be deciphered correctly during Sanger sequencing, leaving an unidentified nucleotide.

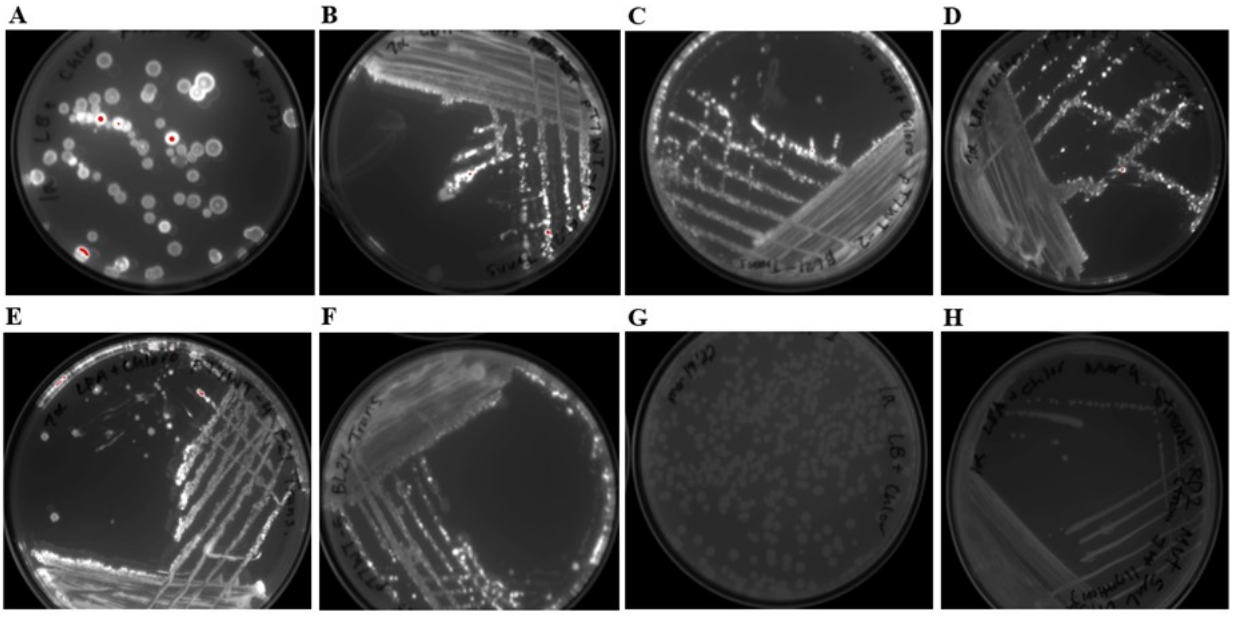

FIG. 4 Leaky GFP expression of the T7 inducible promoter. Images were captured on the BioRad GelDoc UV imaging system using the Alexa458 setting. (**A**) pT71 BL21(DE3) transformation plate. (**B,C,D,E,F**) Master plates of pT71 BL21(DE3) colonies 1-5 restreaked from (A). (**G**) pT7Mut1 BL21(DE3) transformation plate (**H**) Master plate of pT7Mut1 BL21(DE3) colony 1 restreaked from (G). All plates are LB agar with 25μg/mL chlor without IPTG. RFP images not shown due to negligible fluorescence.

the *lacO* sequence of pT71 BL21(DE3) colony 4 (Figure S3A). Thus, sequencing results of pT71 BL21(DE3) colonies show partial presence of the T7 promoter in colonies 2, 3, and 4 (Figure S3). The pT71 BL21(DE3) colony 1 had non-specific sequence results and colony 5 was not submitted for sequencing.

Additionally, the pT7Mut1 and pT7Mut2 BL21(DE3) colonies 1 and 2 contained an intact NruI site and no pT7Mut promoter. This was expected, as the vectors used for transformation of these colonies were from isolated pT7Mut1 and 2 DH5α vectors which also was prior revealed to contain no insert in their sequencing results, corresponding with the gel electrophoresis analysis and the lack of GFP expression detected for all pT7Mut BL21(DE3) colonies (Figure 4G-H, Figure 5).

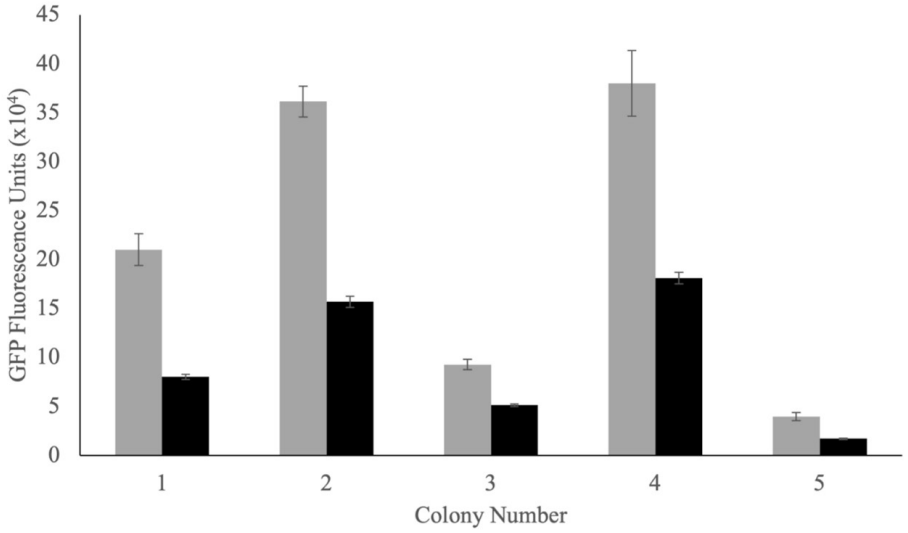

FIG. 5 GFP fluorescence of IPTG induced (gray) and uninduced (black) pT7 BL21(DE3) transformants. A fast IPTG induction protocol was completed using 0.5 mM IPTG substrate incubated in a 37°C for 3 hours. Cell pellets were frozen at -20°C, then later thawed and resuspended in PBS before aliquoting into a 96-well plate. GFP fluorescence measurements were taken using a fluorescence microplate reader at excitation and emission wavelengths of 485 nm and 528 nm, respectively. A PBS blank was subtracted from measurements. The y-axis is shown as GFP fluorescence units divided by a factor of 10,000. Error bars represent standard error (n=2). pT7Mut BL21(DE3) transformants are not shown due to negligible GFP fluorescence for both uninduced and induced cells.

Sequencing results revealed the presence of two HindIII sites in the pSPPH21 empty vector.

Comparing the digested pSPPH21 empty vector in the gel electrophoresis results (Figure 2A), the empty vector appeared to be cut by HindIII. This was unexpected, as the initial analysis of the pSPPH21 empty vector using the SnapGene program did not indicate the presence of HindIII sites (Figure S4A). However, two HindIII sites were found on the pSPPH21 empty vector sequence using the CLC genomics program (Figure S4B). Upon changing the settings of the SnapGene program to show 'All Commercial' enzymes, the two HindIII sites were identified at 1279 bp and 1501 bp within the pSPPH21 vector. Looking at the pT7 sequence with CLC Genomics, one additional HindIII site was identified within the T7 promoter sequence which is expected (Figure S4C). The HindIII sites within the pT7 reference sequence and pSPPH21 vector sequence are separated by approximately 200-270 bp (Figure S4C). Additional DNA fragments after HindIII digestion are likely too small to be resolved in gel electrophoresis, with MW sizes of approximately 200 bp (Figure 2A). Regardless, the incorporated HindIII site in the T7 promoter insert can still be used for insert screening for gel electrophoresis and sequencing analysis as it still produces slight differences in the resulting digested DNA MW. Future investigators should be aware that HindIII also cuts the pSPPH21 empty vector.

UV images of pT7 BL21(DE3) clones showed uninduced basal levels of GFP expression.

Prior to IPTG induction, we wanted to assess whether there was any baseline fluorescent protein expression on transformation plates via the GelDoc imaging system (BioRad) on UV light setting. All colonies were fluorescent on the pT7 plate (Figure 4A), however there were no fluorescent colonies on the pT7Mut plate (Figure 4G). This outcome was as expected based on sequencing results. Five colonies were chosen from the fluorescent pT7 plate, restreaked to create master plates, then imaged using the same system (Figure 4B-F). One colony was restreaked from the non-fluorescent pT7Mut plate for further experiments (Figure 4H). It could not be determined whether the fluorescence was GFP or RFP due to the image being black and white, however prior sequencing results indicated the promoter was in the

forward orientation pertaining to GFP expression. These results suggest that there is leaky GFP expression from the T7 promoter in BL21(DE3) pT7 transformed cells in the absence of the inducer IPTG.

Fast IPTG induction method resulted in greater GFP fluorescence in induced pT7 BL21(DE3) clones compared to uninduced controls.

To assess whether IPTG induction significantly increased baseline levels of GFP or RFP expression, we used a fast induction protocol on pT7 and pT7Mut BL21(DE3) transformants. As a negative control, uninduced pT7 and pT7Mut BL21(DE3) samples were grown alongside IPTG induced samples. As shown in Figure 5, all five uninduced pT7 BL21(DE3) colonies had some level of leaky GFP expression, which was consistent with preliminary imaging results (Figure 4A). All five IPTG induced pT7 clones had significantly increased GFP fluorescence compared to their coinciding uninduced control, based on standard error bars. There was an approximately two-fold increase compared to baseline GFP expression. However, the GFP fluorescence intensity was highly variable, as colonies 2 and 4 had very high GFP expression levels while colony 5 had very low expression levels. RFP fluorescence measurements are not shown due to insignificant fluorescence signals in comparison to the blanks. Measurements of pT7Mut samples are also not depicted for the same reason. These results confirm that there was no RFP expression in pT7 transformed BL21(DE3) nor in pT7Mut clones, as expected by previous sequencing results which illustrated the pT7 clones were inserted in the direction of GFP expression, and pT7Mut clones do not contain the insert. These results also demonstrated that GFP expression was significantly increased with 0.5 mM IPTG induction.

Overnight IPTG induction method resulted in greater GFP fluorescence in uninduced control pT7 BL21(DE3) clones compared to induced clones.

Finally, we tested the same pT7 and pT7Mut BL21(DE3) transformants to further evaluate their fluorescence expression via an overnight induction method using an IPTG concentration gradient. For a negative control, uninduced samples were grown alongside IPTG treated samples. As shown in Figure 6, there were inconsistent trends in the correlation between fluorescence intensity and IPTG concentration. Colonies 1, 2, and 4 have higher GFP fluorescence in uninduced controls than their induced counterparts. In contrast, induced colonies 3 and 5 have similar fluorescence intensities to controls. Measurements involving RFP and pT7Mut were similarly not shown due to negligible fluorescence. Results from this experiment indicate that the basal uninduced expression levels of GFP expression were much greater than when induced with 0.0625-0.5mM IPTG. As such, these results were in disagreement with conclusions from the fast induction experiment and no definite conclusions can be drawn from both IPTG experiments.

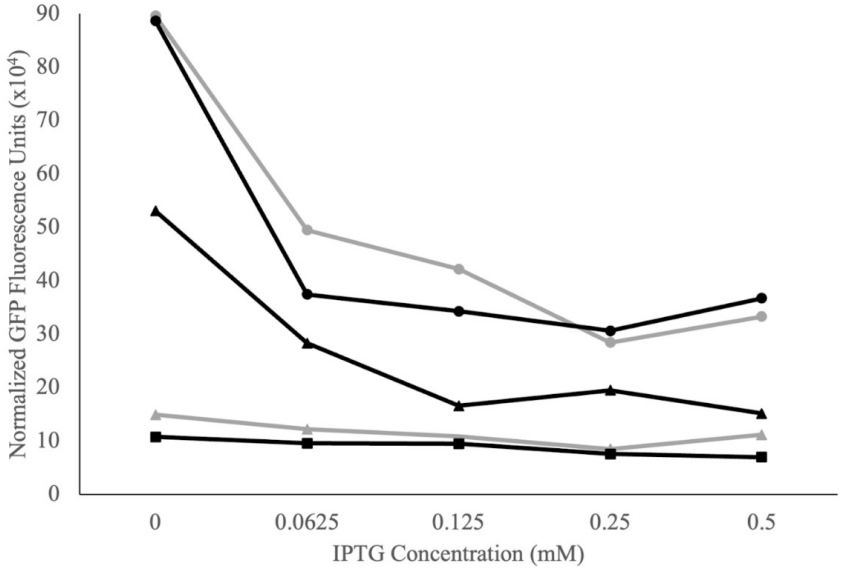

FIG. 6 GFP fluorescence normalized with OD_{600} of overnight IPTG induced pT7 BL21(DE3) transformants at varying concentrations. The overnight IPTG induction occurred within a 96-well plate over a concentration gradient of 0 (control) and 0.5 mM IPTG. Optical density measurements were taken hourly over a 20 hour period using a BioTek microplate reader with orbital shaking at 37°C. The 20 hour OD_{600} readings minus LB broth blanks were used for normalization. GFP fluorescence measurements were taken using a fluorescence microplate reader at excitation and emission wavelengths of 485 nm and 528 nm, respectively. A PBS blank was subtracted from measurements. Colony 1 (black triangle), colony 2 (gray circle), colony 3 (gray triangle), colony 4 (black circle), colony 5 (black square). The y-axis shows GFP fluorescence units divided by a factor of 10,000 (n=2).

This experiment also measured cell density by OD_{600} hourly over 20 hours, shaking at 37°C, to monitor differences in cell growth which may correlate with fluorescence. The growth curve trends of pT7 (Figure S2A-E) and pT7Mut (Figure S2F) appeared to be relatively similar. In Figure S2, growth curves demonstrated similar curves with 0.5 mM IPTG. There were also minimal differences in OD_{600} between induced and uninduced pT7 colonies. However, there was a noticeable difference in three induced pT7 colonies, which exhibited more exponential-like growth than their controls (Figure S2B-D).

DISCUSSION

Blunt end cloning troubleshooting.

Since blunt-end cloning ligates inserts and linearizes without the presence of overhanging bases and the associated hydrogen bond stabilization, it is much less efficient than cohesive-end cloning (16). Although the challenge of generating inserts with complementary ends is no longer present when blunt cloning into a bidirectional vector, empty plasmid recircularization is still a common occurrence (16). To reduce the probability of empty plasmid re-circularizing and increase the number of successful ligations, a few changes were attempted in our own experiments. Firstly, it was suspected that a ligation reaction containing 3:1 ratio of insert to vector had too high of total DNA content. This potentially had an inhibitory effect on the ligation reaction. Furthermore, changing duplex insert to vector ratios to be based on molar ratios rather than concentrations appeared to increase ligation efficiency. Indeed, the 3:1 duplex insert to vector molar concentration ratio granted the best ligation efficiency, confirming our suspicions that the initial total DNA content in the reaction based on DNA concentration was far too excessive. Another suspicion raised was regarding the incubation time; it appeared that a longer incubation time at higher temperature resulted in higher efficiency of positive ligation reactions compared to shorter times. However, the specific time and temperature can still be optimized for better efficiency.

Ligations via blunt-end cloning are dependent on many factors, which make it difficult to pinpoint areas to troubleshoot. It is especially difficult to illustrate what leads to pT7 recombinant plasmids in the direction of GFP, but not in the reverse direction to express RFP. Furthermore, the same difficulties are present in understanding why we were not able to obtain pT7Mut recombinant plasmids. It is suggested that low nucleotide G/C content on the ends of the designed inserts ligate less efficiently compared to other sequences with higher G/C content (17). As such, re-designing the inserts to increase G/C content may help with obtaining recombinant plasmids (Figure 1). Gibson Assembly, a more modern method of blunt-end DNA ligation with higher efficiency compared to traditional blunt-end cloning methods, may also be used in joining the duplex inserts with the linearized plasmid (18). The ligation reaction is streamlined with a single tube reaction using a Gibson Master Mix (19). Gibson assembly is also relatively faster than traditional blunt-end cloning and does not require restriction sites to be present (19). Future attempts with Gibson assembly methods may prove more efficient in ligating desired inserts.

Leaky GFP expression from T7 promoter.

Low levels of GFP expression is to be expected when using a T7 promoter-based system and the respective T7 RNA polymerase, even without the inducer present (20). The T7 RNA polymerase is highly active and has high affinity in transcribing the target genes under the regulation of the T7 promoter (6). Unintended induction may have occurred due to the presence of other sugars such as lactose or galactose, which can induce the lac repressor and consequently unblock transcription under the T7 promoter (6). Similarly, the growth media may supply metabolites that replace the intended induction role of IPTG which result in supposedly uninduced protein expression (6). Some suggested solutions to reduce the basal protein expression levels are growing the cultures in non-inducing growth media, composed of purified components, or supplying growing cultures with T7 lysozyme to remove the unintended expression of T7 RNA polymerase until it is grown in excess during induction (6).

Deletions and rearrangement of pT7 vectors.

Unexpectedly, the isolated and sequenced pT7 recombinant vectors from the BL21(DE3) colonies demonstrated the T7 promoter insert underwent deletions and rearrangements in comparison to the *in silico* sequence (Figure 3). Several hypotheses have been proposed for this phenomenon. First, the sequencing quality of these vectors contained a quality score (QS) ≥ 40 (21). This is a good quality score for Sanger sequencing, which eliminates poor sequencing quality as a possible explanation for these plasmid irregularities. However, this phenomenon could have occurred during the transformation of BL21(DE3) with a mixture of sheared and/or linear pT7 plasmid DNA previously isolated from the pT71 DH5α colony. When transforming cells with linear plasmid DNA, the recircularization of the molecules *in vivo* can lead to deletions and other sequence rearrangements (22). Furthermore, in the process of repeated freeze-thaw cycles, the isolated pT7 plasmid from the pT71 DH5α colony could also have been sheared and linearized (23). The pT7 isolated plasmids may similarly have experienced mechanical stress from processes such as vigorous finger vortexing and the resuspension of plasmid pellets through pipetting during plasmid purification procedures.

These plasmid recombination events could also be due to inherent characteristics of the *E. coli* BL21(DE3) strain, as they express the wild type *endA* and *recA* genes (20). EndA is an endonuclease which cleaves at nonspecific internal sites at both RNA and DNA (24). RecA is a recombinase that promotes genetic recombination (25). These proteins are a constant, but relatively rare, source of recombination errors which can lead to plasmid DNA rearrangements (26). Interestingly, plasmid rearrangement and deletions seen in pT7 only occurred at the point of the T7 promoter insert, with deletions in the T7 promoter and *lacO* sequences, and at the additional HindIII sites (Figure 3). It is possible that EndA and RecA were more active at the insert site where restriction sites such as HindIII or NruI are located. The GFP and RFP gene within the pSPPH21 backbone maintained high sequence identity with the sequenced pT7 BL21(DE3) clones, suggesting there were no rearrangements at the plasmid backbone but only at the insert site (Figure 3). This phenomenon should be further investigated in future experiments.

Lastly, plasmid recombination may have occurred due to plasmid instability from possible toxic gene expression in BL21(DE3) cells. The presence of T7 polymerase, even at basal levels, can lead to the expression of genes in the absence of the inducer (20), as illustrated with our own leaky T7 promoter results. GFP may have toxicity effects on BL21(DE3) cells, especially when overexpressed under extended IPTG induction (27). Thus, extended leaky expression of GFP could have caused plasmid instability and subsequent plasmid rearrangements.

Inconclusive results on the expressional bias between GFP and RFP reporting gene expression.

IPTG induction of pT7 and pT7Mut transformed into BL21(DE3) was done to assess differences in the expression levels between GFP or RFP in the recombinant plasmids. Our results suggest a functional GFP expression system from pSPPH21 with the cloned T7 inducible promoter (Figure 5). Since no RFP expression was reported, no conclusion can be made regarding the functionality or orientation bias of the duo-directional pSPPH21 plasmid.

Discrepancies in the obtained results from different IPTG induction methods reveal potential GFP toxicity

Overall, the induced treatment had lower GFP fluorescence activity compared to the uninduced controls, which was the opposite of what was expected (Figure 6). These unexpected results can be attributed to some GFP toxicity, occurring over a long incubation period. Overexpression of GFP expression has been reported to demonstrate levels of toxicity and interfere with bacterial cell replication (27). In our experiments, the cells were also grown in minimal culture volumes overnight which may potentially incite protein toxicity much faster upon induction with IPTG. Therefore, it is possible that there may have been increased fluorescence activity compared to controls at the beginning of incubation prior to increased toxicity levels, sequestering fluorescent activity. Notably, the tolerance for high levels of toxic proteins may be variable in different bacteria species (27). These results may suggest that the *E. coli* BL21(DE3) strain may be more sensitive to gene expression toxicity, and other

bacterial strains may have more appropriate toxicity thresholds for such experiments involving gene fluorescence.

Defective pT7Mut prompts for further design optimization.

The pT7Mut was expected to induce constitutive fluorescence, however the pT7Mut demonstrated no GFP or RFP expression regardless of IPTG induction in either method. Through screening using gel electrophoresis and Sanger sequencing, it was shown that the T7Mut insert had not ligated into the plasmid, explaining the lack of fluorescence (Figure 4). It is also possible that the mutations introduced into the T7 promoter were functional for constitutive expression of GFP. However, GFP toxicity or the transcription of other byproducts that confer toxicity at very high levels may have occurred, resulting in cell death (27). This cytotoxicity could have resulted in proteases escaping from dead cells, thus leading to the degradation of GFP by the time fluorescence measurements were obtained (27). Another possibility is that the mutations introduced into T7Mut prompted further mutations such as deletions or rearrangements in pT7Mut transformed into BL21(DE3) cells. These mutations could also have caused indirect cytotoxicity through the expression of toxic products (27, 22).

Limitations. The aim of this project was to test the functionality of the GFP and RFP reporter activity in the pSPPH21 plasmid by cloning a T7 promoter-based system and inducing with IPTG substrate. Due to minimal ligation transformants containing the T7 recombinant pSPPH21 plasmid, only a few colonies were analyzed. Only one pT7 DH5α colony demonstrated ligation of the T7 promoter into the pSPPH21 backbone in the orientation which allow GFP expression and creating a pT7 recombinant vector. Transformation using the isolated pT7 recombinant vector resulted in several pT71 BL21(DE3) colonies which demonstrated functional GFP expression and no RFP expression, while the pT7Mut BL21(DE3) colonies did not exhibit any fluorescence activity. As a result, the functionality of the RFP expression in the pSPPH21 plasmid cannot be concluded.

The fast IPTG induction results are also not conclusive because the OD_{600} measurements of the cell culture were not taken prior to fluorescence analysis. As a result, the fluorescence intensity results were not normalized with OD_{600} readings. This may have altered the final fluorescence readings from the IPTG induction experiment since different colonies could be growing at different rates. The leaky expression of the T7 promoter may potentially cause more fluorescence intensity which will increase with cell growth and ultimately contribute to more variability in subsequent fluorescence results. Thus, the fast IPTG induction results are not quantitative, but provide some insight into the functionality of the fluorescence activity.

The fluorescence readings from the overnight IPTG induction experiment were only taken at one time point, which is a study limitation. There was no access to an overnight fluorescence reader to conduct multiple time-point readouts. As such, only an end-point readout after the overnight IPTG incubation period was taken. As previously discussed, there may have been some GFP protein toxicity effect occurring during the incubation period. Therefore, automated tracking of GFP and RFP fluorescence during the IPTG overnight incubation experiment concurrently with OD_{600} could provide greater insight of the hypothetical protein toxicity effects. Additionally, fluorescence measurements at multiple time points could better determine an optimal IPTG incubation time to produce a peak signal.

Conclusions The duo-directional reporter pSPPH21 constructed by Abrishamkar et al. was shown to be functional based on GFP expression when a T7 inducible promoter-based system was inserted in a 5' to 3' direction towards GFP. There was leaky GFP expression from the T7 inducible promoter within the pT7 recombinant plasmid. However, GFP expression was significantly increased through the addition of the IPTG substrate. Further experiments must be performed to determine if RFP or the constitutive T7Mut promoter is functional.

Future Directions. Before pSPPH21 can be used for SIGEX applications, some of the experiments in this project must be repeated and adjusted for clarity and optimization. This includes repeating ligations of the inducible promoters into the pSPPH21 vector to obtain clones with the ligated insert in the reverse direction to express RFP. Furthermore, ligation

conditions must be optimized to obtain a large enough number of clones to gain statistically significant conclusions about insert orientation bias. Since we were not able to obtain any clones with this insert orientation, we were not able to assess RFP functionality or any potential insertion orientation biases of the pSPPH21 vector. To further assess orientation bias after isolating sequenced DH5α transformants with both insert orientations, BL21(DE3) can be transformed with equal quantities of forward and reverse insert plasmid DNA quantities. This should theoretically limit experimental variation and result in approximately 50% GFP and 50% RFP in downstream expression analyses.

It may also be beneficial to redo IPTG induction experiments once RFP expressing clones are obtained in order to quantify both GFP and RFP fluorescence. This could be done through the 96-well plate overnight IPTG induction method. Overnight fluorescence and OD_{600} should be monitored concurrently using a fluorescent plate reader, allowing hourly measurements for both GFP, RFP, and OD_{600} over a 24 hour period. These results would help with understanding why our results unexpectedly showed higher GFP fluorescence for uninduced samples when using this induction method; whether it was due to experimental error or true GFP or IPTG toxicity. This potential cytotoxicity can be evaluated by completing cell viability assays of IPTG induced cell samples at the 24 hour incubation endpoint. Unlike measurements by OD_{600}, this assay enables the differentiation between live and dead cells. Therefore, the percentage of dead cells in induced samples versus induced controls would confirm the presence of cytotoxicity.

Another experimental approach future investigators could take is to design a new inducible promoter that allows for tighter transcriptional regulation of fluorescent protein expression. Including the lac repressor gene (*lacI*) in the insert would result in more repressors present in cells than from the genome of BL21(DE3) cells alone. This would theoretically allow the repressor to bind to the operator at a higher rate, decreasing the leaky fluorescent protein expression from the T7 promoter, as shown in this project.

Lastly, further proof of concept experiments involving screening of metagenomic libraries must be completed before practical use of this duo-directional SIGEX vector. Screening of a defined metagenomic library containing catabolic genes with known substrates would allow for initial assessment of efficiency and practically of this genetic screening system. Once this is completed, pSPPH21 can be used for many applications at higher efficiency levels compared to conventional, unidirectional SIGEX vectors. These applications include identifying novel biocatalysts from unculturable species, or isolating target genes that are difficult to screen through traditional methods (1). SIGEX has recently been used to isolate genes involved in aromatic metabolism from aromatic-hydrocarbon contaminated soil samples, an example of its use in environmental microbiology (28).

ACKNOWLEDGEMENTS

We thank Abrishamkar et al. for constructing the pSPPH21 duo-directional vector and for providing us with a starting point for our project. We also thank Dr. David Oliver, Jade Muileboom and Aditi Nagaraj Nallan for their guidance and support throughout our experiments. This project was funded by the UBC Department of Microbiology and Immunology.

CONTRIBUTIONS

All four members spent approximately 10 hours per week in the UBC Microbiology & Immunology laboratories. Throughout the project, A.B. analyzed all sequencing results. S.A. analyzed fluorescence and microplate data and created associated graphs. A.L. completed background research and wrote the introduction. J.F., A.B., and S.A. collaborated to write materials and methods, create figures, write figure legends, write results, and compile supplemental data. All four group members participated in writing the discussion. Lastly, A.L. completed the abstract and S.A. completed future directions. All group members collaborated to edit the manuscript.

REFERENCES

1. **Uchiyama T, Abe T, Ikemura T, Watanabe K.** 2005. Substrate-induced gene-expression screening of environmental metagenome libraries for isolation of catabolic genes. Nat Biotechnol. **3**(1):88-93. doi: 10.1038/nbt1048
2. **Springer P.** 2000. Gene Traps. Plant Cell. **12**(7):1007-1020. doi: 10.1105/tpc.12.7.1007
3. **Abrishamkar, P, Dana, HM, Oveisi, S, Tabassi, P.** 2021. Construction of SIGEX duo-directional reporter plasmid pSPPH21. Unpublished Manuscript. University of British Columbia.
4. **Seila AC, Core LJ, Lis JT, Sharp PA.** 2009. Divergent transcription: A new feature of active promoters. Cell Cycle, **8**:16, 2557-2564, doi: 10.4161/cc.8.16.9305eila
5. **Tabor S, Richardson C.** 1985. A bacteriophage T7 RNA polymerase/promoter system controlled exclusive expression of specific genes. Proc. Natl. Acad. Sci USA. 82:1074-1078.
6. **Studier W.** 2018. T7 Expression Systems for Inducible Production of Proteins from Cloned Genes in E. coli. Unpublished Manuscript. Brookhaven National Laboratory, U.S. Department of Energy.
7. **Namdev P, Dar H, Srivastava R, Mondal R, Anupam R.** 2019. Induction of T7 Promoter at Higher Temperatures May Be Counterproductive. Indian J Clin Biochem. **34**(3):357-360. doi: 10.1007/s12291-019-0813-y
8. New England BioLabs. 2022. T7 RNA Polymerase.
9. **Betz JL, Sasmor HM, Buck F, Insley MY, Caruthers MH**. 1986. Base substitution mutants of the lac operator: in vivo and in vitro affinities for lac repressor. Gene. (50):123-132.
10. Integrated DNA Technologies, Inc. 2022. Annealing Oligos.
11. **MacWilliams M, Liao M.** 2006. Luria Brother (LB) and Luria Agar (LA) Media and Their Uses Protocol. ASM. n/a.
12. **Chang A, Chau V, Landas J, Pang Y.** 2017. Preparation of calcium competent Escherichia coli and heat-shock transformation. JEMI methods. **1**:22-25.
13. New England BioLabs. 2022. Optimizing Restriction Endonuclease Reactions.
14. New England BioLabs. 2022. Protocol for Dephosphorylation of 5’ -ends of DNA using rSAP (M0371).
15. Biologics International Corp. 2022. IPTG Induction Protocol.
16. Integrated DNA Technologies. 2022. Blunt-end cloning (Cloning strategies, Part 3).
17. Integrated DNA Technologies. 2020. Blunt-end cloning method. Genes & Gene fragments. PDF.
18. **Haseloff J.** 2022. A Guide to Gibson Assembly. University of Cambridge.
19. New England BioLabs. 2022. Gibson Assembly ® Master Mix / Gibson Assembly ® Cloning Kit. Instruction Manual. PDF.
20. ThermoFisher Scientific. 2022. One Shot ™ BL21(DE3)pLysE Chemically Competent E. coli (C656503).
21. Azenta Life Sciences. 2022. Analyzing Sanger Sequencing Data. Technology Spotlight.
22. **Conley E, Saunders V, Saunders J**. 1986. Deletion and rearrangement of plasmid DNA during transformation of Escherichia coli with linear plasmid molecules. Nucleic Acids Research. **14**(22):8905-8917.
23. **Klingström T, Bongcam-Rudloff E, Pettersson O**. 2018. A comprehensive model of DNA fragmentation for the preservation of High Molecular Weight DNA. bioRxiv. doi: 10.1101/254276
24. UniProt Consortium. 2022. UniProtKB - P25736 (END1_ECOLI).
25. **Kuzminov A.** 2013. Recombinational Repair. Brenner’s Encyclopedia of Genetics (Second Edition). 104-108. doi: 10.1016/B978-0-12-374984-0.01284-5.
26. **Al-Allaf F, Tolmachov O, Zambetti L, Tchetchelnitski V, Mehmet H**. 2013. Remarkable stability of an instability-prone lentiviral vector plasmid in Escherichia coli Stbl3. 3 Biotech. **3**(1):61-70. doi: 10.1007/s13205-012-0070-8.
27. **Kain S**. 2006. Methods and Protocols. Green Fluorescent Protein: Properties, Applications, and Protocols, Second Edition. John Wiley & Sons, Inc. 407-421.
28. **Meier M, Paterson S, Lambert I**. 2016. Use of Substrate-Induced Gene Expression in Metagenomic Analysis of an Aromatic Hydrocarbon-Contaminated Soil. Applied Environmental Microbiology, **82**(3):897-909. doi: 10.1128/AEM.03306-15.